

Research Article

Resveratrol potently counteracts quercetin starvation-induced autophagy and sensitizes HepG2 cancer cells to apoptosis.

Sarah Tomas-Hernández¹, Jordi Blanco², Cristina Rojas¹, Joel Roca-Martínez¹, María José Ojeda-Montes¹, Raúl Beltrán-Debón¹, Santiago Garcia-Vallve^{1,4}, Gerard Pujadas^{1,4}, Lluís Arola^{3,4}, Miquel Mulero¹.

¹ Cheminformatic and Nutrition Research Group, Department of Biochemistry and Biotechnology, Rovira i Virgili University, Tarragona, 43007, Spain

² Laboratory of Toxicology and Environmental Health, School of Medicine, IISPV, Universitat Rovira i Virgili, 43201, Reus, Spain

³ Nutrigenomics Research Group, Department of Biochemistry and Biotechnology, Rovira i Virgili University, Tarragona, 43007, Spain

⁴ Technological Unit of Nutrition and Health, EURECAT-Technological Center of Catalonia, Reus, 43204, Spain

Correspondence: Miquel Mulero

E-mail: miquel.mulero@urv.cat

Keywords: Autophagy, AMPK, Apoptosis, HO-1, LMP, p70S6K, Quercetin, Resveratrol.

Abbreviations: **AMPK**, AMP-activated protein kinase; **ER-stress**, endoplasmic-reticulum stress; **HO-1**, heme oxygenase 1; **LC3**, 1A/1B-light chain 3; **LMP**, lysosomal membrane permeabilization; **m-TOR**, mammalian target of rapamycin; **p70S6K**, p70S6 kinase; **QCT**, quercetin; **RSV**, resveratrol; **XBP-1**, X-box binding protein 1.

Received: 19-Jul-2017; Revised: 21-Dec-2017; Accepted: 30-Dec-2017

This article has been accepted for publication and undergone full peer review but has not been through the copyediting, typesetting, pagination and proofreading process, which may lead to differences between this version and the [Version of Record](#). Please cite this article as [doi: 10.1002/mnfr.201700610](https://doi.org/10.1002/mnfr.201700610).

This article is protected by copyright. All rights reserved.

Abstract

Scope: Resveratrol (RSV) has been described as a potent antioxidant, anti-steatotic, and antitumor compound, and it has also been identified as a potent autophagy inducer. On the other hand, quercetin (QCT) is a dietary flavonoid with known antitumor, anti-inflammatory and antidiabetic effects. Additionally, QCT increases autophagy. To study the hypothetical synergistic effect of both compounds, we tested the combined effect of QCT and RSV on the autophagy process in HepG2 cells

Methods and results: Autophagy was studied by western blotting, real-time RT-PCR, and cellular staining. Our results clearly indicate a bifunctional molecular effect of RSV. Both polyphenols were individually able to promote autophagy. Strikingly, when RSV was combined with QCT, it promoted a potent reduction of QCT-induced autophagy and influenced pro-apoptotic signaling.

Conclusion: RSV acts differentially on the autophagic process depending on the cellular energetic state. We further characterized the molecular mechanisms related to this effect, and we observed that AMP-activated protein kinase (AMPK) phosphorylation, heme oxygenase 1 (HO-1) downregulation, lysosomal membrane permeabilization (LMP) and Zinc (Zn^{2+}) dynamics could be important modulators of such RSV-related effects and could globally represent a promising strategy to sensitize cancer cells to QCT treatment.

1 Introduction

Autophagy is a critical intracellular pathway that targets damaged organelles to the lysosome for degradation, and this process is highly conserved in eukaryotic cells [1]. As an initial protective mechanism, autophagy is usually triggered by starvation or damage and functions to maintain cell homeostasis. Degradation of cellular components can entail the uptake of small amounts of cytoplasm at the vacuole or lysosome surface (microautophagy) or, in response to a strong stimulus such as

starvation, the formation of specific double-membrane organelles termed autophagosomes, which engulf larger portions of cytoplasm or organelles before fusing with a vacuole or lysosome (macroautophagy) [2, 3]. Although this process is an important part of the normal balance between anabolism and catabolism and can prolong survival during nutrient deprivation, autophagy is also an alternate death pathway that facilitates type II programmed cell death [4–6]. For this reason, imbalances in this pathway can contribute to diverse pathologies.

Interestingly, the role of autophagy in cancer is quite complicated and controversial. Autophagy is supposed to be tumor suppressive during cancer development but is also thought to contribute to tumor cell survival during cancer progression [7, 8].

Alternatively, autophagy prevents tumor cells from dying by inhibiting apoptosis during nutritional deprivation, and the cells undergo apoptosis when autophagy is prevented [9–11]. Regardless of whether they promote cell survival or cell death, the two processes engage in complex and poorly understood molecular cross-talk [12], and inducing apoptosis and inhibiting protective autophagy have become an effective means of cancer therapy.

Natural compounds are an important source of molecules with interesting health properties and have been widely used for prevention and treatment of metabolic, degenerative and cancer pathologies [13].

Resveratrol (RSV), a phytoalexin found in grape skins, peanuts, and red wine, has been reported to exhibit a wide range of biological and pharmacological properties in several pathological conditions such as fatty-liver [14], inflammation [15] and diabetes [16], among others. Aside from these protective effects, RSV inhibits tumor initiation, promotion and progression in a variety of cell culture systems and animal models by mechanisms that include cell cycle arrest, kinase pathway inhibition and apoptosis activation [17–19]. In addition, RSV-induced autophagy has been suggested to be a key

process in mediating many beneficial effects of RSV, such as reduction of hepatic steatosis, endoplasmic-reticulum stress (ER-stress), inflammation [20, 21] and induction of cancer cell death [7, 22].

On the other hand, quercetin (QCT) is an antioxidative flavonoid that is ubiquitously distributed in plants and is known to have multiple health benefits (i.e., diabetes, inflammation, atherosclerosis and cancer) [23–26]. The anticancer effects of QCT have been attributed to antioxidative activity, inhibition of enzymes, activating carcinogens, modification of signal transduction pathways, and interactions with receptors and other proteins [27]. Moreover, it has also been shown that QCT is able to induce “protective” autophagy in several cancer cell lines [28, 29].

Importantly, the capacity of these compounds to promote cancer cell death that enhances the effects of standard therapies should be taken into consideration for designing novel therapeutic strategies [30]. In this sense, the synergism between autophagy-inducing plant metabolites contained in the diet should not be neglected. By selecting a combination of natural compounds, a better chemosensitization and consequent cell death of cancer cells through autophagic-related mechanisms may be achieved.

The aim of this study was to identify and characterize hypothetical synergistic effects of two well-established natural autophagic inducers, namely RSV and QCT, on autophagy-related mechanisms in HepG2 cancer cells.

2 Materials and Methods

2.1 Chemicals

Resveratrol (RSV) ref. R5010, Quercetin (QCT) ref. Q4951, Thiazolyl Blue Tetra-zolium Bromide (MTT) ref. M5655, Zinc chloride ($ZnCl_2$) ref.96468, as well as the protease inhibitor cocktail ref.

P8340, the phosphatase inhibitor cocktail 2 ref. P5726 and the phosphatase inhibitor cocktail 3 ref. P0044 were obtained from Sigma-Aldrich (St. Louis, USA). Acridine orange (AO) ref. A3568 was obtained from Invitrogen. Dulbecco's modified Eagle's medium (DMEM) was purchased from Lonza (Basel, Switzerland). The human hepatoblastoma HepG2 cell line was obtained from the European Collection of Cell Cultures (Wiltshire, UK).

2.2 Cell culture and general experimental treatment

The human hepatoblastoma HepG2 cells were cultured in 75 cm² flasks (Orange Scientific) with DMEM supplemented with 10% fetal bovine serum, 2% PS (penicillin-streptomycin), 1% L-glutamine, and 1% NEAA (non-essential amino acids) in a humidified atmosphere with 5% CO₂ at 37°C. For the mRNA and protein extraction, cells were seeded at a density of 5×10^5 cells/well in 12-well plates (Orange Scientific). RSV and/or QCT treatments were done by incubating HepG2 cells with increasing concentrations of polyphenols (0, 25, 50 or 100 µM) or a vehicle (0.05% DMSO) and harvesting them at specific time points (0.75, 8 and 24 h). For Zinc (Zn²⁺) experiments, cells were treated (24 h) with fixed concentrations of polyphenols (control, 100 µM QCT, and/or 100 µM RSV) and increasing concentrations of ZnCl₂ (control, 10, 50 or 100 µM).

2.3 MTT assay

Cells were seeded at a density of 5×10^4 cells/well on a 96-well culture plate and incubated overnight. After the treatments, the medium was removed and replaced with 200 µL of fresh medium. Cells were loaded with 50 µL of freshly prepared MTT (5 mg/mL in phosphate buffered saline (PBS)) and incubated for 4 h at 37°C. The blue formazan crystals that formed following the reduction of the MTT

dye were solubilized in 200 μ l of dimethyl sulfoxide (DMSO) and 25 μ l of glycine buffer and quantified using the Helios Zeta UV-VIS ELISA reader (Thermo Scientific). The dye absorbance was measured at a wavelength of 570 nm (680 nm was used as the reference wavelength). The vehicle-treated cells were established as 100% viability. The relative percentage of viability was calculated as follows: Viability (%) = [A570 (compound) / A570 (control)] \times 100. Cell survival or viability (%) was determined by averaging three repeated experiments.

2.4 RNA isolation and cDNA synthesis

Total RNA was obtained from HepG2 cells using a RNeasy Mini Kit (Qiagen, Valencia, CA) according to the manufacturer's protocol. RNA was resuspended in 100 μ L of RNase-free water. The DNase I RNAase-free kit (Fermentas, Thermo Scientific) was used to remove genomic DNA from the RNA preparations. RNA was quantified with a spectrophotometer (Nanodrop 1000 Spectrophotometer, Thermo Scientific) at an absorbance of 260 nm and tested for purity by the A260/280 ratio and for integrity by denaturing gel electrophoresis. The first strand of cDNA was reverse-transcribed from 1 μ g of total RNA from each sample using a First Strand cDNA Synthesis Kit (Fermentas, Thermo Scientific) according to the manufacturer's protocol. An identical reaction without the reverse transcription was performed to verify the absence of genomic DNA.

2.5 Real-time Q-PCR

Quantitative PCR for CHOP, ATF6, ATF4 and cyclophilin was performed using SYBR Premix Ex Taq (Takara) according to the manufacturer's protocol and analyzed on a CFX96 Real-Time PCR Detection System (Bio-Rad, Spain.). The cDNA was amplified using human-specific primers for

CHOP (forward: 5'-AGG GAG AAC CAG GAA ACG GAA ACA-3'; reverse: 5'-TCC TGC TTG AGC CGT TCA TTC TCT-3'), ATF6 (forward: 5'-ATG TCT CCC CTT TCC TTA TAT GGT; reverse: 5'-AAG GCT TGG GCT GAA TTG AA-3'), ATF4 (forward: 5'-GGG TTC TCC AGC GAC AAG GCT AAG-3'; reverse: 5'-AAC AGG GCA TCC AAG TCG AAC TC-3'), and cyclophilin (forward: 5'-TTC ATC TGC ACT GCC AAG AC-3'; reverse: 5'-TCG AGT TGT CCA CAG TAG C-3'). The thermal cycling was composed of an initial step at 50°C for 2 min, followed by a polymerase activation step at 95°C for 10 min and a cycling step with the following conditions: 40 cycles of denaturation at 95 °C for 15 s, annealing at 60°C for 1 min, and extension at 72°C for 1 min. Oligonucleotides of varying lengths produce dissociation peaks at different melting temperatures. Therefore, at the end of the PCR cycles, the PCR products were analyzed using a heat dissociation protocol to confirm that a single PCR product was detected by the SYBR Green dye. The fluorescence data were acquired at the 72°C step. The threshold cycle (Ct) was calculated using the CFX Manager Software to indicate significant fluorescence signals above the noise during the early cycles of amplification. The relative levels of expression of the target genes were measured using cyclophilin mRNA as an internal control according to the $2^{-\Delta\Delta Ct}$ method.

2.6 Analysis of XBP1 mRNA splicing

Spliced XBP1 mRNA induced by activated IRE1 is translated to its protein product, a potent transcription factor that induces BiP/GRP78 expression. XBP1 splicing is also induced by activated ATF6; thus, it is believed to be an important marker reflecting IRE1 and ATF6 signaling in response to ER stress. For this assay, XBP1 cDNA was amplified by PCR using human-specific primers for the XBP1 transcript (forward: 5'-GCT GAA GAG GAG GCG GAA G-3'; reverse: 5'-GTC CAG AAT GCC CAA CAG G-3'). These primers are useful for capturing the XBP1 spliced forms (XBP1s-172

bp amplicon) and the XBP1 unspliced form (XBP1u-197 bp amplicon). The PCR conditions were composed of an initial step at 50 °C for 2 min, followed by a polymerase activation step at 95°C for 10 min and cycling with the following conditions: 40 cycles of denaturation at 95°C for 30 s, annealing at 54°C for 30 sec, and extension at 72 °C for 30 sec. A final extension at 72°C for 10 min was also applied. The PCR products were separated by 4% agarose gel electrophoresis for 280 min and were stained with ethidium bromide.

2.7 Lysosomal membrane stability.

As a marker of lysosomal membrane permeabilization (LMP), the volume of the cellular acidic compartment was visualized by acridine orange (AO) staining. Cells were seeded in six-well tissue culture plates (5×10^5 cells/well). At 24 h following polyphenol treatments, cells were incubated with medium containing 1 $\mu\text{g}/\text{mL}$ AO for 15 minutes. The staining solution was then removed, cells were washed once with PBS, fresh media was added, and fluorescent micrographs were taken using an Olympus inverted fluorescence microscope. All images presented are at the same magnification.

2.8 Western blotting analysis

HepG2 cells were harvested and homogenized in RIPA lysis buffer (50 mM Tris-Cl, pH 7.4, 150 mM NaCl, 1% NP40, and 0.25% Na-deoxycholate, containing protease and phosphatase inhibitors). Aliquots of the cell lysate containing 30 μg of protein per sample were analyzed by western blotting. Briefly, the samples were placed in sample buffer (0.5 M Tris-HCl, pH 6.8, 10% glycerol, 2% (w/v) SDS, 5% (v/v) 2- β -mercaptoethanol, and 0.05% bromophenol blue) and denatured by boiling at 95-100°C for 5 min. The samples were then separated by electrophoresis on 15% polyacrylamide gels.

The proteins were subsequently transferred to polyvinylidene difluoride (PVDF) membranes (Amersham Biosciences, GE Healthcare) using a transblot apparatus (Bio-Rad). The membranes were blocked for 1 h with 5% non-fat milk dissolved in TBS-T buffer (50 mM Tris, 1.5% NaCl, and 0.2% Tween 20, pH 7.5). The membranes were then incubated overnight with primary monoclonal antibodies against cleaved caspase-3 (5A1E; Cell Signaling), eIF2 α (9722; Cell Signaling), phospho-eIF2 α Ser 51 (9721; Cell Signaling), LC3A/B (4108; Cell Signaling), bcl-2 (2876; Cell Signaling), SQTSM1/p62 (88588, Cell Signaling), Beclin 1 (3738, Cell Signaling), phospho-mTOR Ser 2448 (sc-293133; Santa Cruz), phospho-AMPK Thr-172 (2535; Cell Signaling), HO-1 (70081; Cell Signaling), phospho-p70S6 Kinase Thr 389 (9234; Cell Signaling), phospho-S6 Ribosomal Protein Ser 240/244 (2251; Cell Signaling) and β -actin (A 2066; Sigma). The blots were washed thoroughly in TBS-T buffer and incubated for 1 h with a peroxidase-conjugated IgG antibody. The immunoreactive proteins were visualized using an enhanced chemiluminescence substrate kit (ECL plus; Amersham Biosciences, GE Healthcare) according to the manufacturer's instructions. Digital images were obtained with a GBOX Chemi XL 1.4 system (Syngene, UK), which allows for quantification of the band intensity. The protein load was monitored via immuno-detection of actin.

2.8 Docking assay

A docking assay was performed between p70S6 kinase (p70S6K) and two potential inhibitors, RSV and QCT. A subunit of the 3A60 protein structure from PDB was selected for the assay. The protein structure was prepared with Protein Preparation Wizard, and a grid was generated. In protein preparation, the original hydrogens were removed and then added, and missing sidechains and loops were filled in using prime. Ligands were obtained from the ChemSpider database and were prepared

by ligprep to perform the docking. Protein preparation, grid generation and ligprep were carried out using Schrödinger Suite software.

2.9 Statistical analyses

The data were evaluated by Student's T-test or one-way ANOVA, followed by the Bonferroni post hoc tests to identify significant differences between controls and treatments. GraphPad Prism version 6 software was used. Differences were considered significant when the *p* values were less than 0.05. The results are displayed as the mean±SD of at least three independent assays for each experiment.

3 Results

3.1 QCT abrogates RSV-induced ER stress

In our attempt to determine whether polyphenols have a novel synergistic effect, we treated HepG2 cells with several combinations of QCT and RSV for 8 h. Due to our expertise in the field and our previously published [19] and unpublished results, we started to study the consequences of such polyphenol combinations on ER-stress mechanisms. Despite the fact that we have previously shown that RSV induces ER-stress in HepG2 cells [19], the combination of RSV with QCT resulted in significantly lower ER-stress compared to RSV alone. As shown in figure 1, higher doses of RSV promote the splicing of X-box binding protein 1 (XBP-1), a well-established marker of ER-stress activation (figure 1A), and induce C/EBP homologous protein (CHOP) overexpression (figure 1B). In this sense, we observed that high doses of QCT alone do not induce ER-stress, but the combined treatment with RSV results in significantly lower RSV-mediated ER-stress. This effect is also evident when other ER-stress markers were studied, such as eiF2 α phosphorylation and GRP78 and ATF4 expression (figures 1C, D and E, respectively). Interestingly, when we examined the apoptotic pathway using caspase-3 cleavage analysis, we observed the same profile as observed with ER-stress,

indicating that RSV treatment at 8 h induced apoptosis activation, and the combination of RSV with QCT decreased such RSV pro-apoptotic effects (figure 1C). It is noteworthy to mention that the lowest doses of QCT (25 and 50 μ M) had a stronger effect than the highest one (100 μ M).

3.2 RSV silences autophagic activation mediated by QCT

As QCT has been previously described to induce “protective” autophagy [28, 29], we wanted to study the viability of HepG2 cells at 24 h in the presence of high doses of both polyphenols, alone or in combination. As shown in figure 2A, the MTT assay showed that QCT induced a “burst” in HepG2 viability that was counteracted by RSV (RSV 100 μ M + QCT 100 μ M). These viability results were consistent with results obtained when the apoptotic process (via caspase-3 and bcl-2 cleavage) was studied (figure 2B and 2C, respectively). In this sense, we observed a complementary profile to the one obtained with MTT when we studied caspase-3 cleavage, i.e., caspase activation increased when the viability decreased.

Due to the previously observed effect on ER-stress at 8 h, and because the autophagy pathway is intimately associated with the ER-stress process [31], we asked whether the QCT-induced effects on RSV-mediated ER-stress could be related to modulation of the autophagy flux induced by both polyphenols. As seen in figure 2C, both QCT and RSV activated the autophagy process at 24 h, as reflected by the 1A/1B-light chain 3 (LC3) lipidation (LC3-II), with QCT being a more potent activator. This is consistent with previous publications that describe these two polyphenols as autophagy inducers [30, 32, 33].

Surprisingly, despite both polyphenols have been established as autophagy activators, the compounds in combination did not result in a synergistic effect. On the contrary, RSV seemed to act as an

autophagy inhibitor when QCT was present. This was consistent with previously observed effects on the ER-stress process (figure 1A-E). In consequence, it seems that QCT, by inducing the autophagy process, reduced RSV-induced ER-stress in HepG2 cells. On the other hand, RSV suppressed this QCT-mediated autophagy effect, most significantly at the highest dose tested (100 μ M), and was likely responsible for the ER-stress activation.

Consequently, it became clear that the QCT molecular behavior relating to the apoptotic and autophagy processes was different depending on the presence or absence of RSV. Therefore, we focused our efforts on further characterizing this interesting RSV-induced modulation in HepG2 cells. To do so, instead of fixing one polyphenol concentration, we combined three RSV concentrations with three QCT concentrations. Again, as seen in figure 3A and 3B, the autophagy process was decreased when RSV was combined with QCT treatment. More concisely, in figure 3A we can observe higher AO staining, indicating increased acidic vacuoles formation, due to QCT treatment (100 μ M/24 h). In contrast, there was a decrease in staining (red color) in HepG2 cells (acidic vacuoles) induced by RSV co-treatment (100 μ M/ 24 h). This could strongly suggest that RSV co-treatment is inducing LMP.

The level of LC3-II correlates with the number of autophagosomes; therefore, the level of conversion of LC3-I to LC3-II can be used as an indicator for autophagic activity [34] In this sense, figure 3B depicts a decrease in the autophagy marker LC3-II with increasing RSV concentrations at 24 h of treatment.

To further explore the effect of both polyphenols on autophagic flux, we also measured the changes in p62 levels. p62, which is also known as SQSTM1, is an ubiquitin-binding protein that is involved in lysosome- or proteasome-dependent degradation of proteins. It incorporates into the autophagosome via direct interaction with LC3-II and is degraded in the process of autophagy.

Inhibition of autophagy leads to increased levels of p62 [35, 36][36] As shown in Figure 3C, treatment with increasing concentrations of RSV for 24 h resulted in a dose-dependent increase of p62 levels. Furthermore, combination treatment with QCT and increasing concentrations of RSV resulted in a dose-dependent increase of p62 levels compared to either QCT or RSV alone, confirming that RSV inhibits autophagic flux in these hepatoma cells.

Beclin-1 and PI3C3, which form the class III PI3K complex, are involved in the early phase of autophagy. So Beclin-1 can be considered as a biochemical marker of early-stage autophagy. In this sense, as shown in figure 3D, RSV decreases Beclin-1 levels.

In consequence, it must be highlighted that the autophagic flux is decreased by RSV-QCT co-treatment (as indicated by a decrease in LC3-II, Beclin-1; and an increase in SQTSM1/p62), despite the fact that the polyphenol combination inactivated the mammalian target of rapamycin (mTOR), which is the main inhibitory kinase of the autophagic pathway (figure 3E). This suggests that other molecular targets are modulated by RSV and impact inactivation of the autophagy process.

Finally, figure 3F shows that the decrease in autophagy induced by RSV co-treatment triggers potent pro-apoptotic signaling (as signified by the cleavage of caspase-3). It is interesting that, as shown in figure 1B, the increase in the ER-stress-derived pro-apoptotic marker CHOP results in the promotion of caspase-3 cleavage (figure 1C). Consequently, it is likely that the decrease in the autophagy process induced by RSV co-treatment promoted potent pro-apoptotic signaling that could, at least partially, be mediated by increased ER-stress. Nevertheless, we cannot rule out the possibility that QCT in the presence of RSV might also induce more potent apoptotic signaling that might not be related to ER-stress.

3.3 QCT promotes a starvation-like state that is decreased by RSV

To explore the possible molecular mechanisms responsible for modulation of the autophagy process, we treated HepG2 cells for 45 min with QCT and/or RSV and studied several important phosphorylated proteins. Starvation or energy deficiency is one of the hallmarks of autophagy activation. In fact, one of the adaptive pathways induced by the starvation process is AMPK-mediated activation of autophagy in order to obtain energy from this catabolic process [37]. Accordingly, we focused on AMPK phosphorylation. Figure 4A shows that AMPK phosphorylation increased due to QCT treatment. This kinase is activated by a low energetic state of the cell (high 5'-adenosine monophosphate). This suggests that QCT induced a starvation-like state in HepG2 cells that is, at least partially, responsible for induction of autophagy. Interestingly, RSV co-treatment decreased the levels of the phosphorylated form of AMPK. In consequence, it is likely that RSV co-treatment, by counteracting the starvation-like state mediated by QCT, inhibited the autophagic process.

3.4 RSV strongly downregulates hemeoxygenase 1 expression

Hemeoxygenase 1 (HO-1) catalyzes the first and rate-limiting step in heme degradation. Interestingly, evidence accumulated over the past 25 years demonstrates that HO-1 is induced not only by the substrate heme but also by a variety of non-heme inducers such as heavy metals, endotoxins, heat shock, inflammatory cytokines, and prostaglandins. The chemical diversity of HO-1 inducers led to the speculation that HO-1, in addition to its role in heme degradation, may also play a vital function in maintaining cellular homeostasis. Interestingly, HO-1 is also highly induced by a variety of agents causing oxidative stress, and increasing HO-1 expression seems to be protective in animal and in vitro models [38]. Additionally, recent studies have highlighted the critical role of HO-1 in regulating autophagy [39, 40]. Consequently, we focused on the influence of QCT and/or RSV treatments on

HO-1 expression. As shown in figure **4B**, RSV strongly downregulated HO-1 expression in a dose dependent-manner. Furthermore, the highest doses of QCT in combination with RSV slightly reduced this downregulation.

3.5 RSV and QCT inhibit p70S6 Kinase

It has previously been shown that RSV can exert the same “anti-autophagy” and “pro-apoptotic” effect in cells that are under caloric restriction (serum deprivation), and in this case, the postulated mechanism was p70S6K inhibition, a well-known target of mTOR [41]. As a consequence, we were also interested in elucidating if some of the observed effect mediated by RSV was also due to inhibition of this kinase. For this purpose, we studied the phosphorylated state (threonine 389) of p70S6K. We observed that QCT and RSV together or separately resulted in decreased abundance of phosphorylated p70S6K. As previously seen with mTOR, the combination of these polyphenols induced the most potent inhibitory effect on p70S6K phosphorylation (figure **5A**). Interestingly, when we studied the phosphorylation level of S6 ribosomal protein, a well-characterized downstream target of p70S6 kinase, we observed that QCT and/or RSV also strongly reduced the phosphorylation level of S6 ribosomal protein (figure **5B**). Again, the combination of the two polyphenols induced the most potent inhibitory effect on such phosphorylation. This could indicate that both polyphenols are affecting p70S6K function. To further evaluate the effect of these polyphenols on this kinase, we carried out a docking simulation between p70S6K and both compounds. Interactions in the binding site are shown for RSV and QCT (green carbon molecules) with residues (orange carbon molecules) in figure **5C**. Three H bonds (red dashed lines) are predicted for RSV, with Glu143, Leu175 and Asp236. QCT presents the same interactions as RSV and one more, with Lys123. The glide score was

-10,076 for QCT and -6,084 for RSV. This docking assay supports the idea that these polyphenols could be affecting p70S6K function by strongly interacting with its binding site.

3.6 Zn⁺² modulates autophagy and apoptosis induced by QCT and RSV

It has been reported that Zn⁺² could mediate some autophagic processes [42, 43]. In order to preliminarily study if the observed effect of polyphenols on autophagy and apoptosis could be also mediated by Zn⁺² dynamics, we treated HepG2 cells with fixed concentrations of polyphenols (control, 100 μM QCT, and/or 100 μM RSV) and increasing concentrations of ZnCl₂ (control, 10, 50 or 100 μM). Interestingly, as it could be seen in figure 6, autophagy dose-dependently increased by Zn⁺² in the QCT treatments (as indicated by an increase in LC3-II). On the other hand, 10 μM and 50 μM ZnCl₂ increased apoptosis (as indicated by caspase-3 cleavage) in the QCT+RSV treatments. Surprisingly, 100 μM ZnCl₂ decreased apoptosis and increased autophagy in the QCT+RSV condition.

These results suggest that Zn⁺² could influence autophagy and apoptosis induced by QCT and RSV; and, as it will be discussed below, it could be feasible to think that QCT and RSV could be acting as Zn⁺² modulators.

4 Discussion

In this study, we aimed to clarify the interaction of two natural compounds, QCT and RSV, which have been previously described as potent autophagy inducers, in this important catabolic process in HepG2 cells. Unexpectedly, we discovered that the combination of both polyphenols had an opposite

effect on autophagy as well as on ER-stress compared to either of the polyphenols alone. For example, QCT induced a potent activation of autophagy in HepG2 cells that was confirmed through AO staining, Beclin-1 protein expression and conversion of LC3-II (figures 2 and 3). This QCT-mediated activation of autophagy decreased ER-stress induced by RSV (figure 1). On the other hand, RSV also promoted a significant but weaker (compared to QCT) autophagy process (figures 2 and 3). Nevertheless, it seemed that the autophagy induction elicited by both polyphenols was slightly different.

Additionally, QCT promoted a “starvation-like” state characterized by signaling through AMPK that could be, at least partially, responsible for the autophagy induction. Previous research has shown that QCT induces protective autophagy in cancer cells by modulating pathways such as AKT [28], JNK [29] and AMPK [44], among others.

On the other hand, RSV has been shown to induce autophagy by AMPK signaling [45], by SIRT1 induction [46] or by direct inhibition of mTOR through ATP competition [32], among other mechanisms.

Although both compounds did not equally inhibit mTOR phosphorylation (figure 3E); the combination of QCT and RSV induced the most potent inhibition of mTOR phosphorylation. This is important because theoretically, under this molecular scenario (synergistic mTOR inhibition), one would expect that the autophagy process would be exacerbated. In fact, related to this, it has been previously shown that QCT in combination with other substances can potentiate their autophagy- and cell death-inducing qualities [47], and synergisms with other autophagy-inducing natural substances found in plants have been detected [48–50]. This is especially relevant in a nutritional context as QCT is found in numerous foods and is likely to act synergistically with other autophagy-inducing plant metabolites contained in the diet.

Nevertheless, in a cancerous context, such as our HepG2 *in vitro* model or others, QCT in a combined treatment with an autophagy inhibitor may be an excellent therapeutic approach to reduce cancer cell proliferation and could be a promising strategy to sensitize cells to QCT treatment. Several synthetic autophagy inhibitors such as chloroquine [28, 29] and 3-methyladenine [51] have been shown to be successful for this purpose, reducing the “protective” autophagy and maximizing pro-apoptotic cell death.

As far as we know, this is the first report that describes an “antagonistic” effect on the autophagy process caused by two natural autophagy inducers such as QCT and RSV in HepG2 cancer cells. Additionally, this effect seems to be related to the cellular energetic state, due to the differences observed in AMPK phosphorylation between QCT and RSV treatments (figure 4A).

Interestingly, Armour et. al [41], in a series of elegant experiments, showed that RSV suppresses autophagy in a calorie-restricted cellular environment, or by direct mTOR inhibition during rapamycin treatment. Therefore, it is likely that AMPK modulation could play an important role in RSV-mediated effects. Armour and collaborators postulated that the inhibitory effect of RSV on p70S6K was an important factor related to the contrasting effects of RSV on autophagy depending on the nutritional state and hypothesized that insulin signaling could be the key difference. The authors further postulated that under nutrient withdrawal, where insulin signaling was minimal, inhibition of p70S6K induced an autophagy reduction, which could be the primary effect of RSV. Additionally, they also hypothesized that when autophagy was repressed by robust signaling through insulin-PI3K-Akt-mTOR (well-fed state), the disruption of this pathway could lead to the induction of autophagy over time.

We agree with Armour and collaborators that RSV attenuates autophagy, and this could be related to starvation and mTOR inhibition. However, we are also convinced that, in our case, factors other than

p70S6K inhibition are responsible for the observed effects. This is because, as seen in figure 5, we observed that both RSV and QCT seem to inhibit this kinase. Therefore, there must be some differential effect/s of these polyphenols that are responsible for this interesting phenotype in HepG2 cells, and one of these effects could be related to differential modulation of AMPK.

On the other hand, it has been recently shown that either inhibition or siRNA knockdown of HO-1 exacerbates hepatocyte death induced by experimental sepsis *in vivo* or lipopolysaccharide (LPS) treatment *in vitro*, suggesting a pro-survival induction of autophagy via HO-1 action [52]. The same group also demonstrated that in macrophages, LPS induces the release of proinflammatory cytokines with a concomitant increase in autophagy via a toll-like receptor-4 (TLR4)/HO-1-dependent pathway [53]. HO-1 and LC3-II were up-regulated in proximal tubular epithelial cells, using an acute kidney injury model induced by cisplatin, [54]. On the other hand, proximal tubular epithelial cells of HO-1-knockout mice showed significant apoptosis and impaired induction in autophagy [54]. These experiments demonstrated the critical role of HO-1 in the regulation of autophagy. Therefore, in our attempt to identify possible factors that could be characteristic of this RSV suppressive effect on autophagy, we focused on HO-1 modulation due to QCT and/or RSV treatment.

HO-1, known to be an anti-oxidative molecule, is the first and rate-limiting enzyme in the catabolism of heme, producing equimolar amounts of biliverdin, CO, and free iron. In addition, HO-1 is highly induced under stress conditions. Human HO-1 deficiency increases sensitivity to oxidative stress, resulting in severe endothelial damage. The influence of polyphenols on HO-1 has also been widely studied [55–57], but little is known about its relationship to autophagy regulation. In this sense, our results (figures 4B) clearly show that RSV strongly downregulated HO-1 protein content, and this correlates with the anti-autophagic effect of RSV. Consistent with our results, it has been shown that the HO-1 inhibitor zinc protoporphyrin (ZnPP) strongly inhibits autophagy and induces apoptosis [58] and that HO-1 induces protective autophagy [40].

Additionally, as Zn^{+2} has been intimately associated with autophagic processes [42, 43], we have also explored the hypothetical role of this metal in the observed molecular effect of RSV and QCT in our in vitro HepG2 model. In this sense, we have used $ZnCl_2$ as a source of Zn^{+2} at several concentrations (0 μM , 10 μM , 50 μM and 100 μM of $ZnCl_2$). As observed in figure 6, the autophagic activity (LC3 turnover) induced by QCT seems to be increased by Zn^{+2} . Interestingly, the polyphenol combination (QCT+RSV) abrogates autophagy at 0 μM , 10 μM and 50 μM of $ZnCl_2$, but it induces a slight increase in autophagy process at the higher concentration (100 μM $ZnCl_2$). This later effect of QCT+RSV combination correlates with an increase in the caspase-3 cleavage, except for the last condition (100 μM $ZnCl_2$), where the slight activation of autophagy coincides with a slight decrease on caspase-3 activation. In consequence, it is feasible to hypothesize that, at the higher Zn^{+2} dose, some kind of polyphenol-mediated effect/s on Zn^{+2} dynamics seem to be saturated; reactivating, in consequence, the autophagy process in HepG2 and decreasing the caspase-3 cleavage. Interestingly, it has been previously shown that QCT can act as Zn^{+2} ionophore in Hepa cancer cells [59]; and on the other hand, by using a liposome model it has also been shown that RSV and QCT are able to differentially modulate Zn^{+2} dynamics [60]. Nevertheless, more experiments are needed to further clarify this interesting Zn^{+2} -mediated effect.

In conclusion, QCT can induce protective autophagy in HepG2 cells. It is reasonable to think that under mTOR inhibition or caloric restriction, RSV could act as an autophagy suppressor instead of behaving as an autophagy inducer, thereby sensitizing cells to QCT treatment. Additionally, because autophagy induced by QCT or RSV is negatively regulated by mTOR, and both polyphenols inhibit p70S6K, we hypothesize that other factors are responsible for this characteristic and differential effect. In view of our results, we propose that in this context (polyphenol co-treatment) RSV acts as an autophagy inhibitor or blocker by at least modulating AMPK phosphorylation levels and downregulating HO-1 expression. Additionally, our AO results suggest that RSV is affecting the

lysosomal membrane stability. In this sense, it has been previously shown by other authors that RSV induced lysosome leakage [61, 62]. Furthermore, RSV mediated autophagy and apoptosis in cervical cancer cells was related with RSV-mediated cathepsin-L release from the lysosomes [63]. So, it is feasible to think that in our experimental model, at least, some part of the pro-apoptotic signaling could be also mediated also by cathepsin release. In this sense, in the QCT+RSV condition it would be likely that QCT is “loading” HepG2 cells with AV (autophagolysosomes) that are permeated by RSV. Thus, blocking the autophagic flux (SQSTM1/p62 accumulation) and liberating, as a consequence of such LMP, its harmful content to the cytosol (inducing a potent pro-apoptotic effect). This would also explain why despite the fact that the maximal mTOR inhibition occurs in the QCT+RSV condition we observe a significant decrease or blockade on the autophagy process.

We cannot rule out the idea that other important molecular mechanisms related to autophagy might also be modulated by the polyphenol combination. For example, it could be possible that in this context (polyphenol co-treatment), RSV sensitizes HepG2 cancer cells to apoptosis by inhibiting the QCT-induced mitophagy of organelles that are a signal for apoptotic cell death

Nevertheless, we are very conscious that further experiments are required to validate all these hypotheses.

Finally, we suggest that the application of combinations of QCT and RSV in the treatment of other cancer cells or tumor models could be an interesting area for further study. Additionally, it will be interesting to test the effects of RSV on autophagy in animals, especially under starvation, mTOR inhibition or tumor models, where we may observe a similar duality of function induced by RSV.

Author contributions: M.M designed the research and wrote the manuscript, S.TH conducted the research and wrote the manuscript. J.RM conducted the docking assay. All authors read and approved the final manuscript.

Acknowledgements: ST-H's contract was supported by grant 2012BPURV_30 from our University. MJO-M's contract was supported by grants 2014PFR-URV-B2-67 and 2015PFR-URV-B2-67 from our University. MM is a Serra Hünter Associate Professor. This manuscript was edited for English language fluency by American Journal Experts

The authors declare that they have no conflicts of interest.

5 References

- [1] Levine, B., Klionsky, D.J., Development by Self-Digestion. *Dev. Cell* 2004, 6, 463–477.
- [2] Reggiori, F., Klionsky, D.J., Autophagy in the eukaryotic cell. *Eukaryot. Cell* 2002, 1, 11–21.
- [3] Lum, J.J., DeBerardinis, R.J., Thompson, C.B., Autophagy in metazoans: cell survival in the land of plenty. *Nat. Rev. Mol. Cell Biol.* 2005, 6, 439–48.
- [4] Tsujimoto, Y., Shimizu, S., Another way to die: autophagic programmed cell death. *Cell Death Differ.* 2005, 12 Suppl 2, 1528–34.
- [5] Shintani, T., Klionsky, D.J., Autophagy in health and disease: a double-edged sword. *Science* 2004, 306, 990–5.
- [6] Rubinsztein, D.C., Gestwicki, J.E., Murphy, L.O., Klionsky, D.J., Potential therapeutic applications of autophagy. *Nat. Rev. Drug Discov.* 2007, 6, 304–12.
- [7] Miki, H., Uehara, N., Kimura, A., Sasaki, T., Yuri, T., Yoshizawa, K., Tsubura, A., Resveratrol induces apoptosis via ROS-triggered autophagy in human colon cancer cells. *Int. J. Oncol.* 2012, 40, 1020–8.
- [8] Yang, Z., Klionsky, D.J., Mammalian autophagy: core molecular machinery and signaling

- regulation. *Curr. Opin. Cell Biol.* 2010, 22, 124–31.
- [9] Boya, P., González-Polo, R.-A., Casares, N., Perfettini, J.-L., Dessen, P., Larochette, N., Métivier, D., Meley, D., Souquere, S., Yoshimori, T., Pierron, G., Codogno, P., Kroemer, G., Inhibition of macroautophagy triggers apoptosis. *Mol. Cell. Biol.* 2005, 25, 1025–40.
- [10] Hippert, M.M., O'Toole, P.S., Thorburn, A., Autophagy in cancer: good, bad, or both? *Cancer Res.* 2006, 66, 9349–51.
- [11] Lum, J.J., Bauer, D.E., Kong, M., Harris, M.H., Li, C., Lindsten, T., Thompson, C.B., Growth factor regulation of autophagy and cell survival in the absence of apoptosis. *Cell* 2005, 120, 237–48.
- [12] Maiuri, M.C., Zalckvar, E., Kimchi, A., Kroemer, G., Self-eating and self-killing: crosstalk between autophagy and apoptosis. *Nat. Rev. Mol. Cell Biol.* 2007, 8, 741–52.
- [13] Newman, D.J., Cragg, G.M., Natural products as sources of new drugs over the 30 years from 1981 to 2010. *J. Nat. Prod.* 2012, 75, 311–35.
- [14] Ajmo, J.M., Liang, X., Rogers, C.Q., Pennock, B., You, M., Resveratrol alleviates alcoholic fatty liver in mice. *Am. J. Physiol. Gastrointest. Liver Physiol.* 2008, 295, G833–G842.
- [15] Das, S., Das, D.K., Anti-inflammatory responses of resveratrol. *Inflamm. Allergy Drug Targets* 2007, 6, 168–73.
- [16] Szkudelski, T., Szkudelska, K., Anti-diabetic effects of resveratrol. *Ann. N. Y. Acad. Sci.* 2011, 1215, 34–9.
- [17] Ulrich, S., Wolter, F., Stein, J.M., Molecular mechanisms of the chemopreventive effects of resveratrol and its analogs in carcinogenesis. *Mol. Nutr. Food Res.* 2005, 49, 452–61.

- [18] Kotha, A., Sekharam, M., Cilenti, L., Siddiquee, K., Khaled, A., Zervos, A.S., Carter, B., Turkson, J., Jove, R., Resveratrol inhibits Src and Stat3 signaling and induces the apoptosis of malignant cells containing activated Stat3 protein. *Mol. Cancer Ther.* 2006, 5, 621–9.
- [19] Rojas, C., Pan-Castillo, B., Valls, C., Pujadas, G., Garcia-Vallve, S., Arola, L., Mulero, M., Resveratrol enhances palmitate-induced ER stress and apoptosis in cancer cells. *PLoS One* 2014, 9, e113929.
- [20] Ji, G., Wang, Y., Deng, Y., Li, X., Jiang, Z., Resveratrol ameliorates hepatic steatosis and inflammation in methionine/choline-deficient diet-induced steatohepatitis through regulating autophagy. *Lipids Health Dis.* 2015, 14, 134.
- [21] Zhang, Y., Chen, M., Zhou, Y., Yi, L., Gao, Y., Ran, L., Chen, S., Zhang, T., Zhou, X., Zou, D., Wu, B., Wu, Y., Chang, H., Zhu, J., Zhang, Q., Mi, M., Resveratrol improves hepatic steatosis by inducing autophagy through the cAMP signaling pathway. *Mol. Nutr. Food Res.* 2015, 59, 1443–57.
- [22] García-Zepeda, S.P., García-Villa, E., Díaz-Chávez, J., Hernández-Pando, R., Gariglio, P., Resveratrol induces cell death in cervical cancer cells through apoptosis and autophagy. *Eur. J. Cancer Prev.* 2013, 22, 577–84.
- [23] Mahmoud, M.F., Hassan, N.A., El Bassossy, H.M., Fahmy, A., Quercetin protects against diabetes-induced exaggerated vasoconstriction in rats: effect on low grade inflammation. *PLoS One* 2013, 8, e63784.
- [24] Li, Y., Yao, J., Han, C., Yang, J., Chaudhry, M.T., Wang, S., Liu, H., Yin, Y., Quercetin, Inflammation and Immunity. *Nutrients* 2016, 8, 167.
- [25] Hung, C.-H., Chan, S.-H., Chu, P.-M., Tsai, K.-L., Quercetin is a potent anti-atherosclerotic

- compound by activation of SIRT1 signaling under oxLDL stimulation. *Mol. Nutr. Food Res.* 2015, *59*, 1905–17.
- [26] Srivastava, S., Somasagara, R.R., Hegde, M., Nishana, M., Tadi, S.K., Srivastava, M., Choudhary, B., Raghavan, S.C., Quercetin, a Natural Flavonoid Interacts with DNA, Arrests Cell Cycle and Causes Tumor Regression by Activating Mitochondrial Pathway of Apoptosis. *Sci. Rep.* 2016, *6*, 24049.
- [27] Murakami, A., Ashida, H., Terao, J., Multitargeted cancer prevention by quercetin. *Cancer Lett.* 2008, *269*, 315–25.
- [28] Wang, K., Liu, R., Li, J., Mao, J., Lei, Y., Wu, J., Zeng, J., Zhang, T., Wu, H., Chen, L., Huang, C., Wei, Y., Quercetin induces protective autophagy in gastric cancer cells: involvement of Akt-mTOR- and hypoxia-induced factor 1 α -mediated signaling. *Autophagy* 2011, *7*, 966–78.
- [29] Kim, H., Moon, J.Y., Ahn, K.S., Cho, S.K., Quercetin induces mitochondrial mediated apoptosis and protective autophagy in human glioblastoma U373MG cells. *Oxid. Med. Cell. Longev.* 2013, *2013*, 596496.
- [30] Hasima, N., Ozpolat, B., Regulation of autophagy by polyphenolic compounds as a potential therapeutic strategy for cancer. *Cell Death Dis.* 2014, *5*, e1509.
- [31] Rashid, H.-O., Yadav, R.K., Kim, H.-R., Chae, H.-J., ER stress: Autophagy induction, inhibition and selection. *Autophagy* 2015, *11*, 1956–1977.
- [32] Park, D., Jeong, H., Lee, M.N., Koh, A., Kwon, O., Yang, Y.R., Noh, J., Suh, P.-G., Park, H., Ryu, S.H., Resveratrol induces autophagy by directly inhibiting mTOR through ATP competition. *Sci. Rep.* 2016, *6*, 21772.

- [33] Zhao, Y., Fan, D., Zheng, Z.-P., Li, E.T.S., Chen, F., Cheng, K.-W., Wang, M., 8-C-(E-phenylethenyl)quercetin from onion/beef soup induces autophagic cell death in colon cancer cells through ERK activation. *Mol. Nutr. Food Res.* 2017, *61*, 1600437.
- [34] Mizushima, N., Yoshimori, T., Levine, B., Methods in mammalian autophagy research. *Cell* 2010, *140*, 313–26.
- [35] Klionsky, D.J., Abeliovich, H., Agostinis, P., Agrawal, D.K., Aliev, G., Askew, D.S., Baba, M., Baehrecke, E.H., Bahr, B.A., Ballabio, A., Bamber, B.A., Bassham, D.C., Bergamini, E., Bi, X., Biard-Piechaczyk, M., Blum, J.S., Bredesen, D.E., ... Deter, R.L., Guidelines for the use and interpretation of assays for monitoring autophagy in higher eukaryotes. *Autophagy* 2008, *4*, 151–175.
- [36] Mizushima, N., Yoshimori, T., How to interpret LC3 immunoblotting. *Autophagy* 2007, *3*, 542–5.
- [37] Hardie, D.G., AMPK and autophagy get connected. *EMBO J.* 2011, *30*, 634–5.
- [38] Choi, A.M., Alam, J., Heme oxygenase-1: function, regulation, and implication of a novel stress-inducible protein in oxidant-induced lung injury. *Am. J. Respir. Cell Mol. Biol.* 1996, *15*, 9–19.
- [39] Dong, C., Zheng, H., Huang, S., You, N., Xu, J., Ye, X., Zhu, Q., Feng, Y., You, Q., Miao, H., Ding, D., Lu, Y., Heme oxygenase-1 enhances autophagy in podocytes as a protective mechanism against high glucose-induced apoptosis. *Exp. Cell Res.* 2015, *337*, 146–59.
- [40] Surolia, R., Karki, S., Kim, H., Yu, Z., Kulkarni, T., Mirov, S.B., Carter, A.B., Rowe, S.M., Matalon, S., Thannickal, V.J., Agarwal, A., Antony, V.B., Heme oxygenase-1-mediated autophagy protects against pulmonary endothelial cell death and development of emphysema

- in cadmium-treated mice. *Am. J. Physiol. Lung Cell. Mol. Physiol.* 2015, 309, L280-92.
- [41] Armour, S.M., Baur, J.A., Hsieh, S.N., Land-Bracha, A., Thomas, S.M., Sinclair, D.A., Inhibition of mammalian S6 kinase by resveratrol suppresses autophagy. *Aging (Albany. NY)*. 2009, 1, 515–28.
- [42] Liuzzi, J.P., Guo, L., Yoo, C., Stewart, T.S., Zinc and autophagy. *Biometals* 2014, 27, 1087–96.
- [43] Hwang, J.J., Kim, H.N., Kim, J., Cho, D.-H., Kim, M.J., Kim, Y.-S., Kim, Y., Park, S.-J., Koh, J.-Y., Zinc(II) ion mediates tamoxifen-induced autophagy and cell death in MCF-7 breast cancer cell line. *Biometals* 2010, 23, 997–1013.
- [44] Chen, B.-L., Wang, L.-T., Huang, K.-H., Wang, C.-C., Chiang, C.-K., Liu, S.-H., Quercetin attenuates renal ischemia/reperfusion injury via an activation of AMP-activated protein kinase-regulated autophagy pathway. *J. Nutr. Biochem.* 2014, 25, 1226–1234.
- [45] Wu, Y., Li, X., Zhu, J.X., Xie, W., Le, W., Fan, Z., Jankovic, J., Pan, T., Resveratrol-activated AMPK/SIRT1/autophagy in cellular models of Parkinson's disease. *Neurosignals.* 2011, 19, 163–74.
- [46] Ma, L., Fu, R., Duan, Z., Lu, J., Gao, J., Tian, L., Lv, Z., Chen, Z., Han, J., Jia, L., Wang, L., Sirt1 is essential for resveratrol enhancement of hypoxia-induced autophagy in the type 2 diabetic nephropathy rat. *Pathol. Res. Pract.* 2016, 212, 310–8.
- [47] Jakubowicz-Gil, J., Langner, E., Wertel, I., Piersiak, T., Rzeski, W., Temozolomide, quercetin and cell death in the MOGGCCM astrocytoma cell line. *Chem. Biol. Interact.* 2010, 188, 190–203.

- [48] Mertens-Talcott, S.U., Talcott, S.T., Percival, S.S., Low concentrations of quercetin and ellagic acid synergistically influence proliferation, cytotoxicity and apoptosis in MOLT-4 human leukemia cells. *J. Nutr.* 2003, *133*, 2669–74.
- [49] Mertens-Talcott, S.U., Bomser, J. a, Romero, C., Talcott, S.T., Percival, S.S., Ellagic acid potentiates the effect of quercetin on p21waf1/cip1, p53, and MAP-kinases without affecting intracellular generation of reactive oxygen species in vitro. *J. Nutr.* 2005, *135*, 609–14.
- [50] Mertens-Talcott, S.U., Percival, S.S., Ellagic acid and quercetin interact synergistically with resveratrol in the induction of apoptosis and cause transient cell cycle arrest in human leukemia cells. *Cancer Lett.* 2005, *218*, 141–51.
- [51] Chang, J.-L., Chow, J.-M., Chang, J.-H., Wen, Y.-C., Lin, Y.-W., Yang, S.-F., Lee, W.-J., Chien, M.-H., Quercetin simultaneously induces G0 /G1 -phase arrest and caspase-mediated crosstalk between apoptosis and autophagy in human leukemia HL-60 cells. *Environ. Toxicol.* 2017.
- [52] Carchman, E.H., Rao, J., Loughran, P.A., Rosengart, M.R., Zuckerbraun, B.S., Heme oxygenase-1-mediated autophagy protects against hepatocyte cell death and hepatic injury from infection/sepsis in mice. *Hepatology* 2011, *53*, 2053–62.
- [53] Waltz, P., Carchman, E.H., Young, A.C., Rao, J., Rosengart, M.R., Kaczorowski, D., Zuckerbraun, B.S., Lipopolysaccharide induces autophagic signaling in macrophages via a TLR4, heme oxygenase-1 dependent pathway. *Autophagy* 2011, *7*, 315–20.
- [54] Bolisetty, S., Traylor, A.M., Kim, J., Joseph, R., Ricart, K., Landar, A., Agarwal, A., Heme oxygenase-1 inhibits renal tubular macroautophagy in acute kidney injury. *J. Am. Soc. Nephrol.* 2010, *21*, 1702–12.

- [55] Liu, S., Hou, W., Yao, P., Li, N., Zhang, B., Hao, L., Nüssler, A.K., Liu, L., Heme oxygenase-1 mediates the protective role of quercetin against ethanol-induced rat hepatocytes oxidative damage. *Toxicol. In Vitro* 2012, 26, 74–80.
- [56] Fernández-Iglesias, A., Quesada, H., Díaz, S., Pajuelo, D., Bladé, C., Arola, L., Josepa Salvadó, M., Mulero, M., DHA sensitizes FaO cells to tert-BHP-induced oxidative effects. Protective role of EGCG. *Food Chem. Toxicol.* 2013, 62, 750–7.
- [57] Kim, H.-S., Quon, M.J., Kim, J.-A., New insights into the mechanisms of polyphenols beyond antioxidant properties; lessons from the green tea polyphenol, epigallocatechin 3-gallate. *Redox Biol.* 2014, 2, 187–95.
- [58] Wang, Y., Xiong, X., Guo, H., Wu, M., Li, X., Hu, Y., Xie, G., Shen, J., Tian, Q., ZnPP reduces autophagy and induces apoptosis, thus aggravating liver ischemia/reperfusion injury in vitro. *Int. J. Mol. Med.* 2014, 34, 1555–64.
- [59] Dabbagh-Bazarbachi, H., Clergeaud, G., Quesada, I.M., Ortiz, M., O’Sullivan, C.K., Fernández-Larrea, J.B., Zinc ionophore activity of quercetin and epigallocatechin-gallate: from Hepa 1-6 cells to a liposome model. *J. Agric. Food Chem.* 2014, 62, 8085–93.
- [60] Clergeaud, G., Dabbagh-Bazarbachi, H., Ortiz, M., Fernández-Larrea, J.B., O’Sullivan, C.K., A simple liposome assay for the screening of zinc ionophore activity of polyphenols. *Food Chem.* 2016, 197, 916–923.
- [61] Boya, P., Kroemer, G., Lysosomal membrane permeabilization in cell death. *Oncogene* 2008, 27, 6434–51.
- [62] Trinchero, N.F., Nicotra, G., Follo, C., Castino, R., Isidoro, C., Resveratrol induces cell death in colorectal cancer cells by a novel pathway involving lysosomal cathepsin D. *Carcinogenesis*

2006, 28, 922–931.

- [63] Hsu, K.-F., Wu, C.-L., Huang, S.-C., Wu, C.-M., Hsiao, J.-R., Yo, Y.-T., Chen, Y.-H., Shiau, A.-L., Chou, C.-Y., Cathepsin L mediates resveratrol-induced autophagy and apoptotic cell death in cervical cancer cells. *Autophagy* 2009, 5, 451–60.

Graphic Abstract

In a cancerous context, such as HepG2 in vitro model or others, quercetin (QCT) in a combined treatment with an autophagy inhibitor, may be an excellent therapeutic approach to reduce cancer cell proliferation and could be a promising strategy to sensitize cells to QCT treatment. In this sense, several synthetic autophagy inhibitors such as chloroquine or 3-methyladenine have been shown to be successful for this purpose (reducing the “protective” autophagy induced by QCT and maximizing the pro-apoptotic cell death). In this research paper we have described that Resveratrol (RSV) will act differentially on the autophagy process depending on the cellular energetic state. We have further characterized the molecular mechanisms that are related to this effect and we have observed that the AMP activated protein kinase (AMPK) phosphorylation and heme oxygenase 1 (HO-1) downregulation, Lysosome membrane permeabilization (LMP) and Zn^{2+} could be important modulators of such RSV related effect, and could globally represent a promising strategy to sensitize cancer cells to QCT treatment

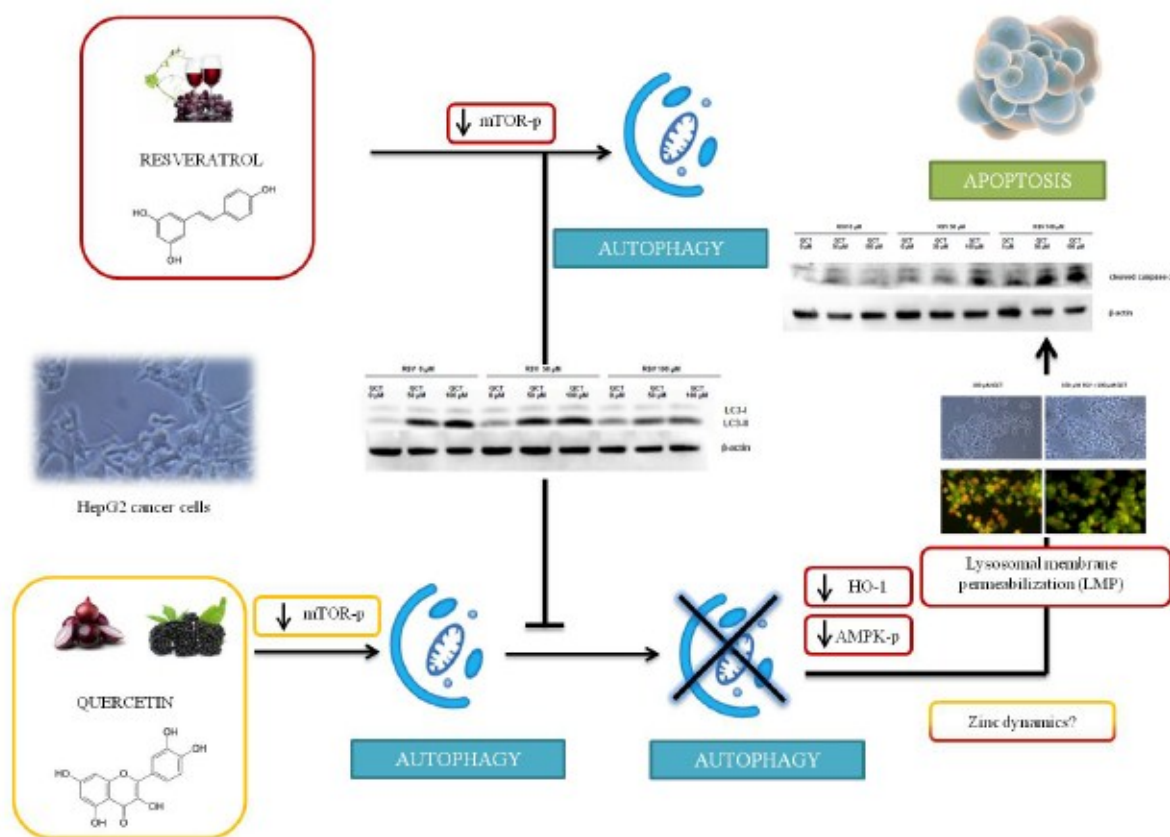


Figure legends

Figure 1. QCT inhibited RSV-induced ER-stress in HepG2 cells. After HepG2 cells were treated with several concentrations of RSV and/or QCT for 8 h, cell lysates were collected and proteins and mRNA were extracted. **(A)** The spliced form of XBP-1 analyzed by PCR and gel electrophoresis. **(B)** CHOP mRNA expression analyzed by real-time RT-PCR. **(C)** Phosphorylation level of eiF2 α analyzed by western blotting using total eiF2 α or β -actin as the reference protein. **(D)** GRP78 mRNA expression analyzed by real-time RT-PCR. **(E)** ATF4 mRNA expression analyzed by real-time RT-PCR. **(F)** Cleaved-caspase 3 level analyzed by western blotting using β -actin as the reference protein. For western blotting and XBP-1 splicing results, one representative image of three independent experiments is shown. For real-time RT-PCR results and densitometry, data are expressed as the mean \pm SD of three independent experiments. Differences relative to the control (a) or to the 100 μ M RSV condition (b) were analyzed by one-way ANOVA followed by the Bonferroni post hoc test. The results were considered significant when $p < 0.05$.

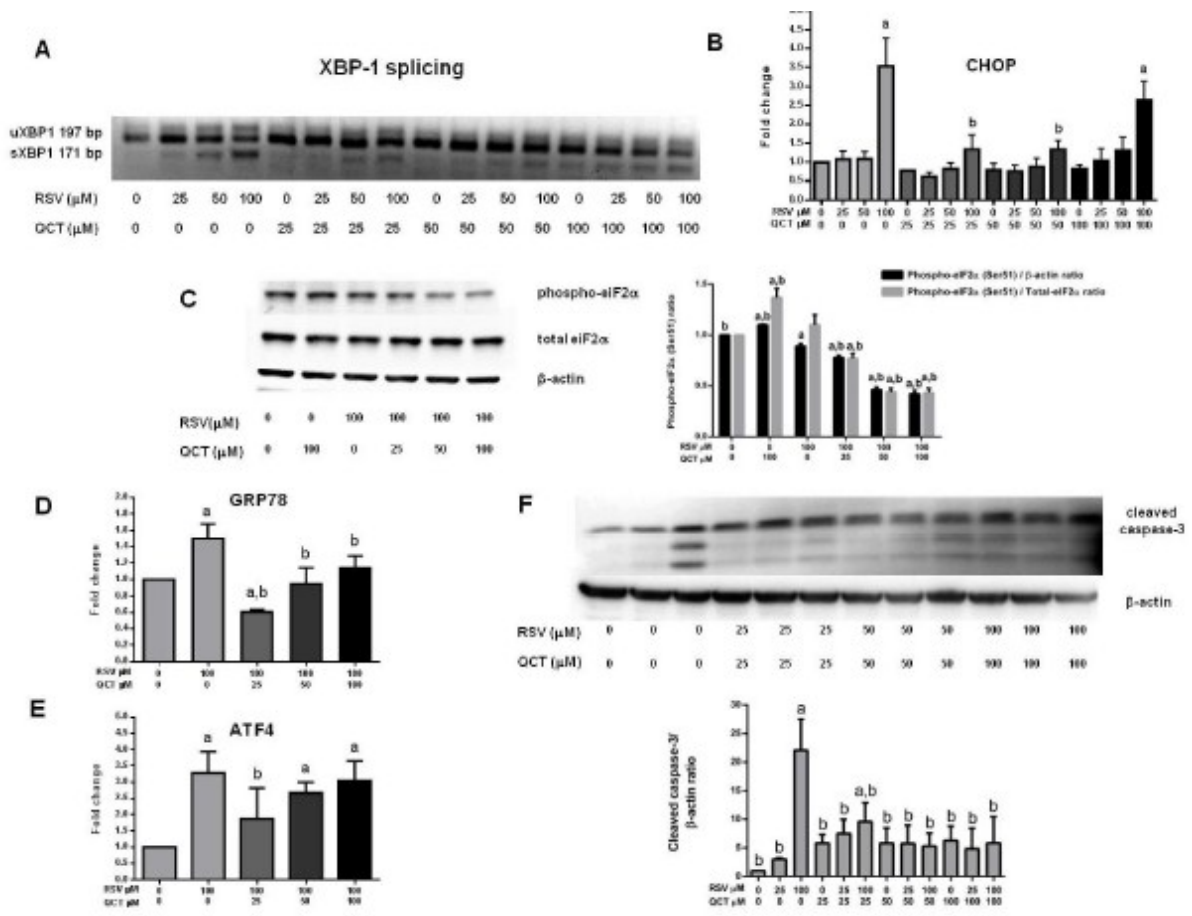
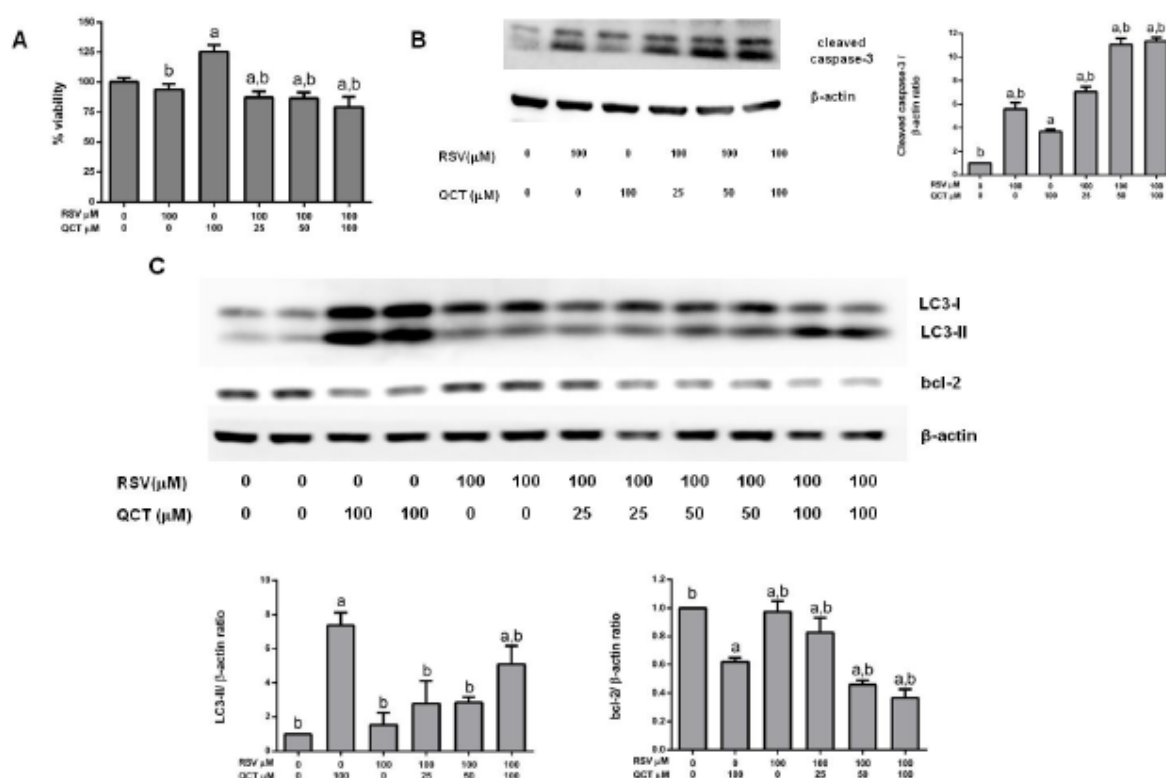
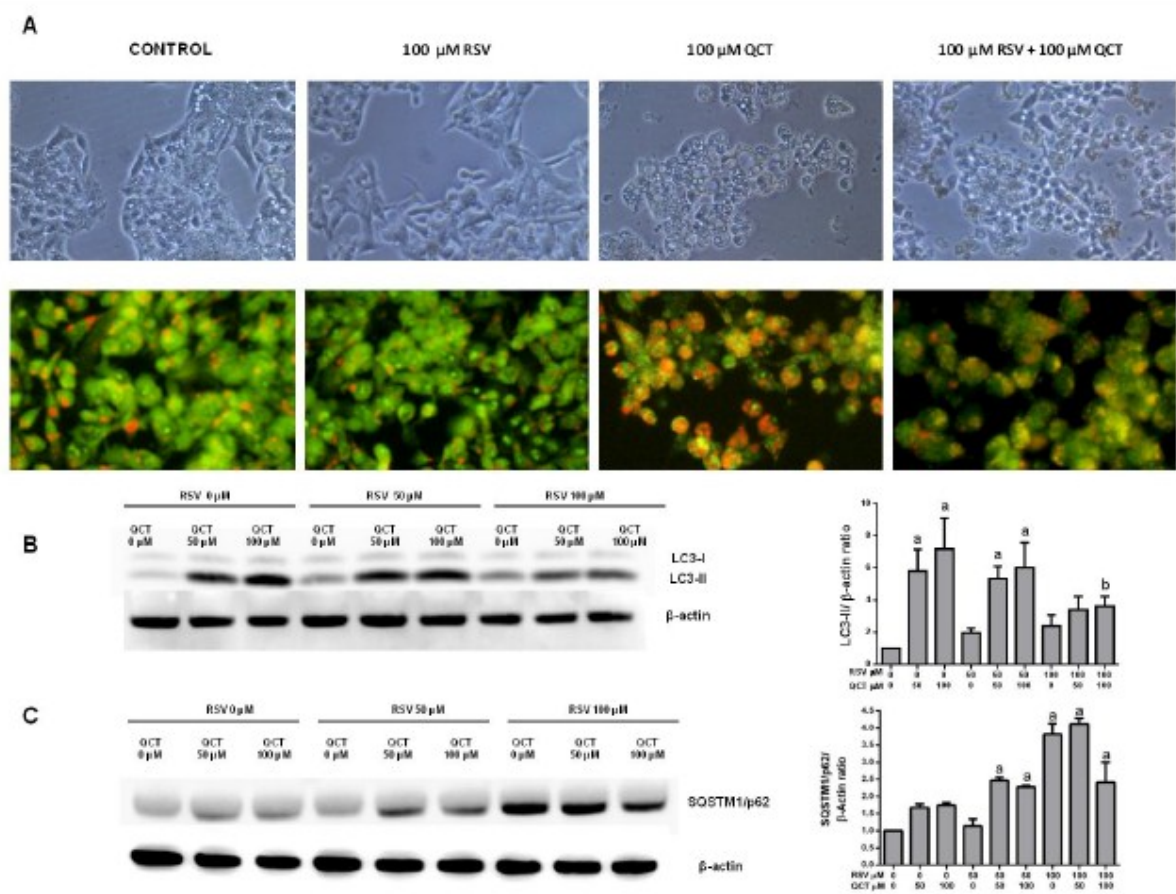


Figure 2. QCT induced a protective autophagy that was decreased by RSV. After HepG2 cells were treated with several concentrations of RSV and/or QCT for 24 h, cell viability was assessed by MTT and cell lysates were collected for western blotting. **(A)** HepG2 viability evaluated using the MTT assay. Data are shown as the mean \pm SD of three independent experiments. **(B)** Cleaved caspase-3 analysis by western blotting. The blot shown is a representative image of three independent experiments. **(C)** LC3-II and bcl-2 levels were analyzed by western blotting using β -actin as the reference protein. One representative image of three independent experiments is shown. For all densitometry tests, differences relative to the control (a) or to the 100 μ M QCT condition (b) were analyzed by one-way ANOVA followed by the Bonferroni post hoc test. Results were considered significant when $p < 0.05$.



This article is protected by copyright. All rights reserved.

Figure 3. RSV abrogated QCT-induced autophagy despite mTOR inhibition. After HepG2 cells were treated with several concentrations of RSV and/or QCT for 24 h, fluorescent images were acquired and cell lysates were collected for western blotting. **(A)** AO staining. One representative image of 10 images per condition is shown. All images presented are at the same magnification. **(B)** LC3-II and bcl-2 levels were analyzed by western blotting using β -actin as the reference protein. One representative image of three independent experiments is shown. Band densitometry is shown on the right. **(C)** SQSTM1/p62 levels were analyzed by western blotting using β -actin as the reference protein. One representative image of three independent experiments is shown. Band densitometry is shown on the right. **(D)** Beclin-1 levels were analyzed by western blotting using β -actin as the reference protein. One representative image of three independent experiments is shown. Band densitometry is shown on the right. **(E)** Phospho-mTOR (Ser 2448) levels were analyzed by western blotting using β -actin as the reference protein. One representative image of three independent experiments is shown. Band densitometry is shown on the right. **(F)** Cleaved caspase-3 analysis by western blotting. The blot shown is a representative image of three independent experiments. Band densitometry is shown on the right. For all densitometry tests, differences relative to the control were analyzed by one-way ANOVA followed by the Bonferroni post hoc test. Results were considered significant when $p < 0.05$.



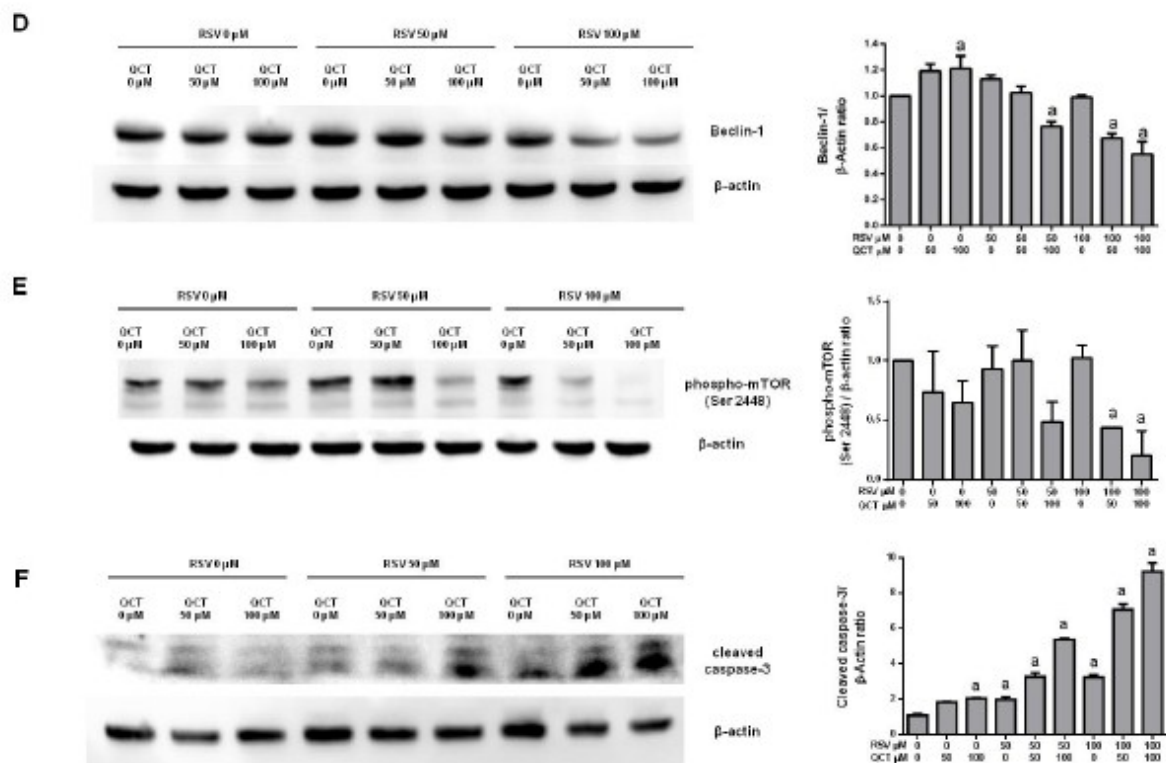


Figure 4. AMPK phosphorylation and HO-1 expression were related to the RSV autophagy inhibition effect. After HepG2 cells were treated with several concentrations of RSV and/or QCT for 45 min, cell lysates were collected for western blotting. **(A)** phospho-AMPK (Thr 172) levels analyzed by western blotting using β -actin as the reference protein. One representative image of three independent experiments is shown. Band densitometry is shown on the right. **(B)** HO-1 analysis by western blotting. The blot shown is a representative image of three independent experiments. Band densitometry is shown on the right. For all densitometry tests, differences relative to the control (a) or to the 100 μ M QCT condition (b) were analyzed by one-way ANOVA followed by the Bonferroni post hoc test. The results were considered significant when $p < 0.05$.

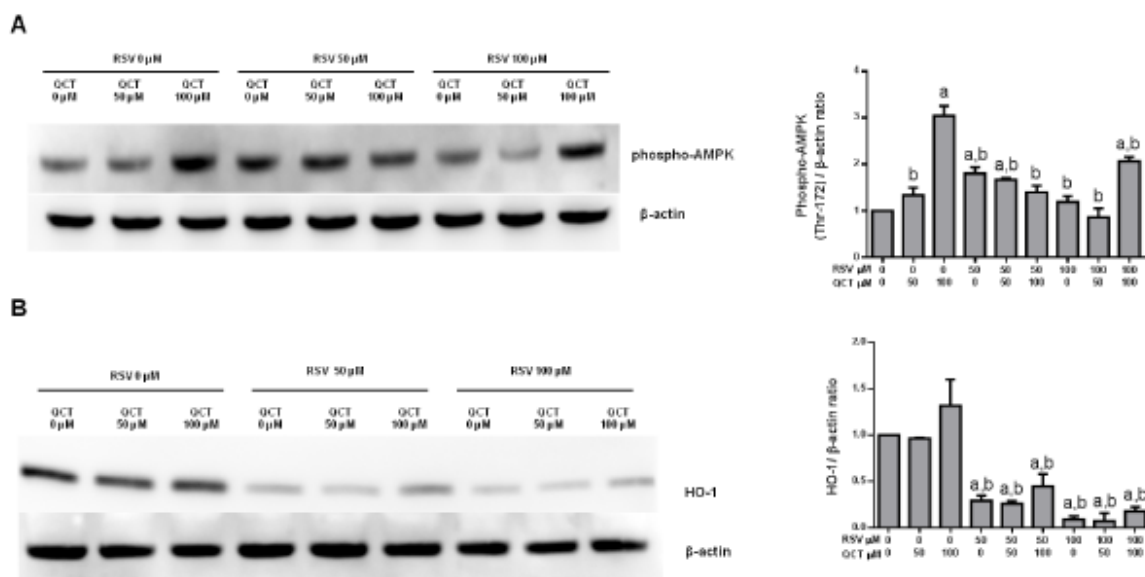


Figure 5. p70S6 kinase was inhibited by QCT and RSV. After HepG2 cells were treated with several concentrations of RSV and/or QCT for 45 min, cell lysates were collected for western blotting. **(A)** Phospho-p70S6 kinase (Thr 389) levels analyzed by western blotting using β -actin as a reference protein. One representative image of three independent experiments is shown. Band densitometry is shown on the right. **(B)** Phospho-S6 ribosomal protein (Ser 240/244) analysis by western blotting. The blot shown is a representative image of three independent experiments. Band densitometry is shown on the right. For all densitometry tests, differences relative to the control (a) were analyzed by one-way ANOVA followed by the Bonferroni post hoc test. Results were considered significant when $p < 0.05$. **(C)** Docking assay of QCT and RSV with p70S6 kinase.

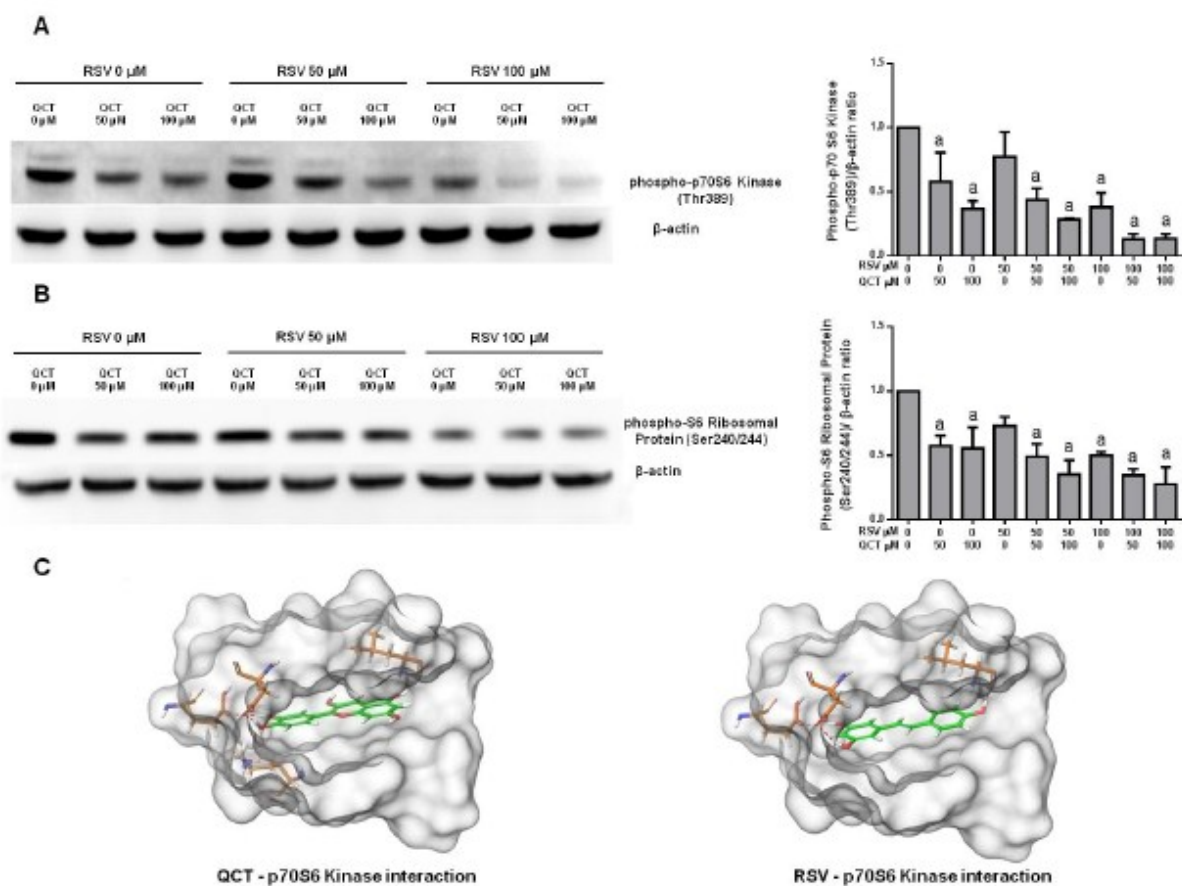
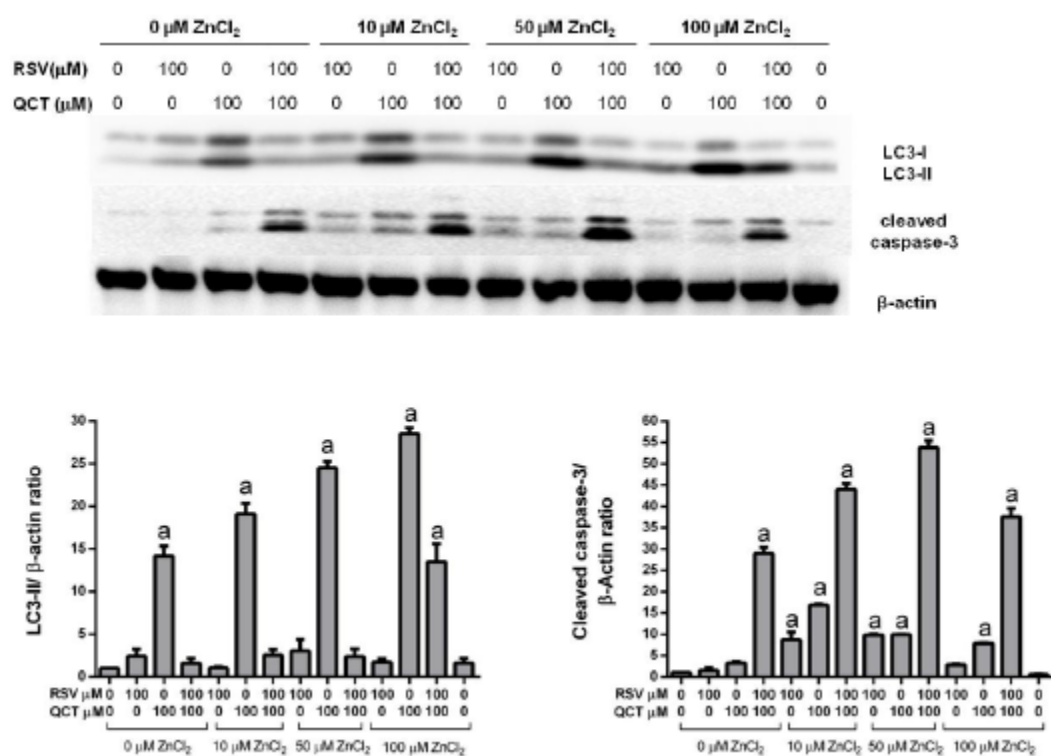


Figure 6. Zn²⁺ influences QCT and RSV effects on autophagy and apoptosis. HepG2 cells were treated with fixed concentrations of polyphenols (control, 100 μ M QCT, and/or 100 μ M RSV) and increasing concentrations of ZnCl₂ (control, 10, 50 or 100 μ M) for 24h. LC3-II and cleaved caspase-3 levels were analyzed by western blotting using β -actin as the reference protein. One representative image of three independent experiments is shown. Band densitometry is shown below. For all densitometry tests, differences relative to the control (a)-were analyzed by one-way ANOVA followed by the Bonferroni post hoc test. Results were considered significant when $p < 0.05$.



This article is protected by copyright. All rights reserved.